

# EFFECT OF DEPTH OF CORRELATION ON CROSS-CORRELATION BLOOD FLOW MEASUREMENTS IN GLASS MICROCHANNELS

*Boris Chayer<sup>1</sup>, Jacques A. de Guise<sup>2</sup> and Guy Cloutier<sup>1</sup>*

<sup>1</sup> Laboratory of biorheology and medical ultrasonics, University of Montreal Hospital Research Center, Montreal, Canada; <sup>2</sup> Laboratory of imaging and orthopedics, University of Montreal Hospital Research Center, Montreal, Canada

## ABSTRACT

The aim of this study was to evaluate the effect of the depth of correlation (DOC) on the cross-correlation method (CC) applied to microcirculatory blood flow in vitro. The cross-correlation algorithm was optimized to compute red blood cell velocity profiles in tube flow. Flow rates, estimated by computing the circular integral of mean velocity profiles, were compared with calibrated pump flows for different focus planes of the microscope and different flow rates. Results show a mean flow underestimation of  $2.8 \pm 5\%$  for all positions of the focus plane inside the tube diameter, highlighting the non-negligible DOC effect when CC is applied to study blood microcirculation. An underestimation of 1% was found with an optimal focus plane. To conclude, flow rate estimation in microcirculatory blood flow can be accurate if the DOC effect is properly compensated for by the CC flow estimation method.

**Index Terms** — red blood cells, out-of-focus microscopy, intravital microscopy, blood flow estimation, microvessels.

## 1. INTRODUCTION

The cross-correlation method (CC) is a technique largely used to study fluid behavior in intravital microscopy and in microelectromechanical systems. For applications to investigate microcirculatory blood flow, it is important to understand the effect of out-of-focus particles on the estimation of velocities. The cross-correlation of two consecutive images is a general method used to calculate particle velocities. An interrogation window in the first image is compared with an interrogation window grid in the second image to find particle displacements. The distance between the center of both windows can be divided by the time elapse between each frame to calculate the mean velocity of particles for this position. Even if CC is a flexible and robust method [1], the CC algorithm needs to be validated for applications dealing with a high seeding volume of cells as in microcirculatory blood flow.

Optical microscopic concepts such as the depth of field and resolution concern the sharpness of an object. However,

in image processing one has to consider superimposed objects that may be out-of-focus. Under these conditions, blurred particles (i.e., blood cells) may affect velocities computed with CC algorithms. The depth of correlation (DOC) is a relatively new concept in microscopy that takes into account the manner in which the image is built and used [2]. It describes how far one particle, over or under the focal plane, affects image-processing algorithms and can be interpreted as a measurement of spatial resolution in the Z dimension. DOC is mainly proportional to the diameter of the particle in flow and inversely proportional to the microscopic lens aperture. Most microparticle image velocimetry ( $\mu$ PIV) studies investigated sub-micron particles [3] with very low seeding volume to reduce the DOC effect and to minimize disturbances when assessing fluid behavior. These images are slightly affected by DOC in that spatial resolution in Z dimension stays small in regard to channel depth. In blood microcirculation study, red blood cells (RBCs) are the particles of interest, and the impact of DOC becomes complicated as RBCs are relatively large in size ( $\approx 7 \mu\text{m}$  in diameter) and because the seeding volume is also important (the physiological hematocrit or volume fraction of RBCs in blood is typically between 20 to 50%). With a DOC as large as the size of microvessels to be studied, which may vary from 15 to 100  $\mu\text{m}$  in the microcirculation, flowing blood may look like fuzzy moving speckles (e.g., see Fig. 2). The depth-averaging effect attributed to the DOC can thus lead to biased estimates between real particle velocities and speckle velocities on the image. Consequently, RBCs in the center stream of blood vessels have higher velocities than measured speckle velocities on flow images.

Several techniques were adopted to overcome the optical DOC limitation, namely nanoparticle seeding in blood [4], fluorescent labeling of a sub-fraction of RBCs [5], base clipping filtering [6] and blood dilution [7]. A major disadvantage, however, is that these techniques can affect the physiological flowing behavior of blood. This is why CC studies of blood at a physiological hematocrit need a better understanding of the effect of the image formation on velocity assessments.

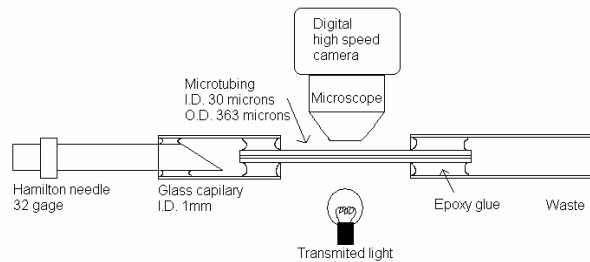


Figure 1: Schematic of the microcirculation in vitro set up with a 30  $\mu\text{m}$  inner diameter glass tubing.

In the current study, DOC was measured experimentally and the effect of flowing out-of-focus particulates at a high seeding volume was highlighted. An in vitro model was built to reproduce typical images of flowing whole blood in the microcirculation. The flow rate in the tube was determined from the mean velocity profile and compared with that of a calibrated syringe pump.

## 2. MATERIALS AND METHODS

### 2.1. In vitro model

An in vitro model of the microcirculation was built with a 30  $\mu\text{m}$  inner diameter and 363  $\mu\text{m}$  outer diameter fused silica tubing (no. 062801, SGE Inc, Austin, TX, USA), glued with Epoxy in 1 mm inner diameter glass capillaries at both ends (Fig. 1). A 10  $\mu\text{L}$  microsyringe connected to a 32 gage needle (no. 7635-01, Hamilton, Reno, NV, USA) was glued at one end of the model to allow perfusion of the microtube with minimal dead volume between it and the needle. The syringe was fixed on a computer-controlled syringe pump to inject blood into the microcirculation model at a constant flow rate ranging from 1 to 27  $\mu\text{L}/\text{h}$ . Blood flow images were acquired with an Axiotech Vario microscope (Zeiss, Oberkochen, Germany) equipped with a 40X water immersion lens (NA. 0.8) in transmission light mode. A 0.63X C-mount adaptor allowed the recording of image sequences via a high-speed digital camera (no. 1M150, Dalsa, Waterloo, Ontario, Canada). The camera, connected to a digital frame grabber (model Hélios, Matrox, Montreal, Qc, Canada), could record up to 2,000 frames / s at a resolution of 120 by 170 pixels with a calibrated isotropic pixel width of 0.42  $\mu\text{m}$ . Image sequences were post-processed with a two-dimensional cross-correlation algorithm developed in Matlab (ver. 7 R14, Natick, MA, USA).

### 2.2. Experimental set up to evaluate DOC

An experimental way of visualizing the DOC is by fixing some RBCs on a microscope slide and finding the range where out-of-focus cells are still visible. Focus plane position is then recorded from the microscope-focusing planetary for different images above and under the optimal focus plane.

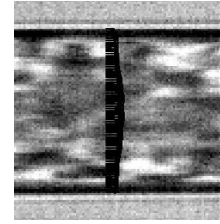


Figure 2: Typical image of blood flow with the in vitro model for a flow rate of 22  $\mu\text{L}/\text{h}$  and the velocity vectors of the mean velocity profile (MVP)

### 2.3. Blood preparation

Two different blood preparations were tested in the model to validate the image processing algorithm with aggregating and non-aggregating RBCs. Blood samples from a healthy adult were collected in heparinized tube, centrifuged, and the buffy coat and plasma were separated from sedimentated RBCs by aspiration. Non-aggregating washed blood samples were prepared by resuspending RBCs at 45% hematocrit in physiological saline solution. Aggregating blood samples were produced by resuspending RBCs at 45% hematocrit in plasma without the buffy coat. Figure 2 presents a typical microscopic image obtained with non-aggregating RBCs.

### 2.4. Computation of RBC velocities

Because RBCs at a physiological hematocrit are not distinguishable on microscopic images (e.g., Fig. 2), the speckle size was used to ascertain the dimension of correlation windows. That size was set by an empirical method that allowed to determine particle displacements for the range of flow rates considered in this study. Square windows were chosen instead of rectangular ones to facilitate eventual application of the algorithm on tortuous real vessels. The size of the first correlation window was set to 15 by 15 pixels, and the size of the second interrogation window was 60 by 60 pixels. An overlap of 100% minus one pixel was chosen to get a high density of velocity vectors (Fig. 2) because the often used sampling with 50% overlap would only provide 10 speed vectors for the width of the glass microvessel in Fig. 1. Oversampling was helpful in this study, as it allowed narrow-band filtering to decimate spurious vectors created by noisy images. A median filter was employed to reject all vectors with a module or angle different from the median value plus one standard deviation computed from all vectors on the same stream line. In addition, a mean filter was used on 50 successive images with the hypothesis that for a given point in an image, velocity is supposed to be constant in time because a steady flow pump was utilized to circulate blood. By using both filtering strategies (median filter and time mean filter), a mean velocity profile (MVP) was determined for each video sequence, as shown in Fig. 3 for a flow rate of 22  $\mu\text{L}/\text{h}$ , an hematocrit of non-aggregating RBCs of 45% and acquisition at the optimum focus plane.

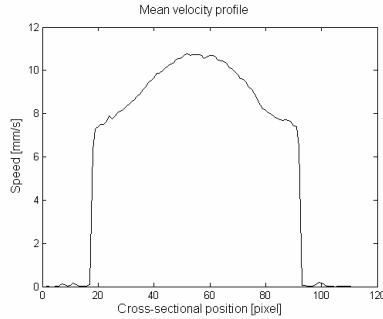


Figure 3: Typical MVP obtained by the mean cross correlation of 50 successive images at a flow rate of 22  $\mu\text{L/h}$ . Non-aggregating RBCs at a hematocrit of 45% was used and the frame rate of the camera was 2,000 images / s.

## 2.5. Estimation of blood flow

To validate the precision of the algorithm and to assess its sensitivity to out-of-focus particles, estimated flows were compared with flows of the pump for a wide range of blood flows and focal planes within the tube. MVP represents the temporal mean speed of particles, with Eq. 1, it allowed to estimate the flow rate  $Q$  produced by the pump.

$$Q = \pi \int_{-r}^{+r} MVP dr \quad (1)$$

As MVP extended out of the microtube because of the relatively large correlation windows of our microscopic images, velocity profiles were limited to the dimension of the tube to reduce errors in flow estimation.

## 3. RESULTS

### 3.1. Effect of DOC on microscopic slide

The focus plane positions for image series showed on Fig. 4 were, from left to right, -64  $\mu\text{m}$  and -24  $\mu\text{m}$  (images A and B), 0  $\mu\text{m}$  (image C), and +12  $\mu\text{m}$  and +44  $\mu\text{m}$  (images D and E). Images A and E show the maximum distance where RBCs could be seen. If we consider images B and D as the limit where the intensity of RBC speckle is consistent enough to modify the result of the cross correlation for MVP estimation, then the DOC is from 24  $\mu\text{m}$  above to 12  $\mu\text{m}$  under the optimal focus plane (i.e. an experimental DOC of 36  $\mu\text{m}$ ). According to Meinhart et al., DOC for a RBC is theoretically 27.6  $\mu\text{m}$  when observed with a 40X, NA 0.8 microscope lens [2].

### 3.2. Effect of DOC on flow estimation

The effect of DOC on flow estimation is presented in Fig. 5. The focus plane of the microscope was changed to image the in vitro model perfused with blood at a constant flow rate of 5  $\mu\text{L/h}$ . The illustration shows that the flow evaluation is close to the expected value even when the

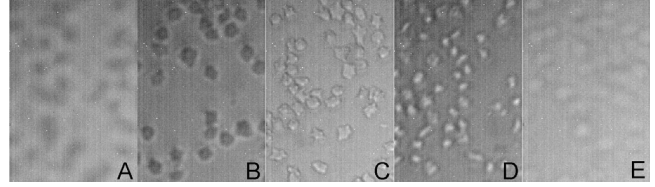


Figure 4: RBCs on a microscope slide at different focus planes. From left to right, 64 and 24  $\mu\text{m}$  above the optimum focus plane, at the center, and 12 and 44  $\mu\text{m}$  under it.

focus plane is not perfectly at the middle of the tube. The circle on the graph corresponds to the inside diameter of the tube. It can be seen that flow estimations have a mean precision of  $97.2 \pm 5\%$  (mean  $\pm$  std) for all focus planes included inside of the tube diameter.

### 3.3. Validity of the 2D cross-correlation algorithm to estimate flow in the in vitro model

Flow estimation was compared with pump flow that was varied from 1 to 27  $\mu\text{L/h}$ . Results are presented in Fig. 6. Each data point is the mean of 5 estimated flows. A good correspondence was obtained for both blood types. The mean error dispersion was 2.3% for the entire range of flow, showing that the cross correlation is a good tool to evaluate physiological blood flow despite the fact that DOC affects the RBC image formation. Linear regressions between experimental and theoretical results showed correlations above 98%. Slight underestimations of the flow by 1% and 3% for washed and reconstituted bloods were found, respectively. The Reynolds number of the aggregating blood solution ranged between  $5.4$  and  $9.5 \times 10^{-2}$  suggesting laminar flow. The pseudo-shear rate at the selected flow rate of 5  $\mu\text{L/h}$  was  $350 \text{ s}^{-1}$ . According to Fung [8], a pseudo shear rate of  $20 \text{ s}^{-1}$  inhibits aggregation, consequently our experiments with aggregating and non-aggregating blood exhibited similar behaviors.

## 4. DISCUSSION

Microscopic slide images (Fig. 4) revealed that the DOC for blood is larger than the expected theoretical one. Even if it is difficult to judge when RBCs are out of focus enough to not affect the correlation algorithm, our results showed a wide range of focus planes for which good flow estimates were obtained (Fig. 5). The DOC plays a role in image formation and, consequently, on the accuracy of image processing algorithms, but the effect appeared maximized when microvessels smaller than the DOC were considered.

Furthermore, a non-symmetrical DOC effect was observed above and below the focal plane, which differs from the symmetry predicted by the DOC theory but agrees with the work of Parthasarathi et al. on in vivo hamster microvessel [9]. It is important to note that the DOC theory is built on the hypothesis of low spherical seeding particles

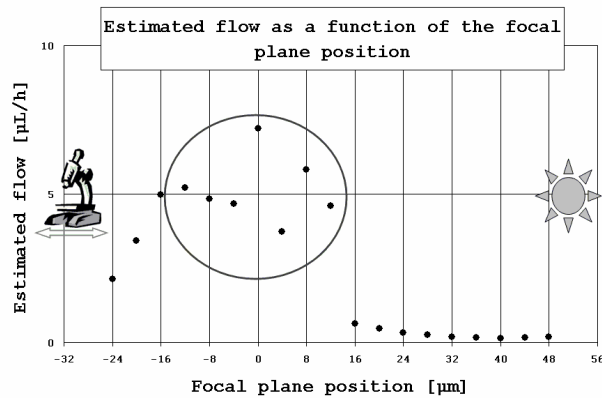


Figure 5: In vitro blood flow estimation for different focus planes. Blood hematocrit and flow rate were constant at 45% and 5  $\mu\text{L}/\text{h}$ , respectively. The circle on the graph corresponds to the inside diameter of the tube.

in fluid as usually used in  $\mu\text{PIV}$ . The fact that blood is a fluid with a high-seeding density of cells and the non spherical shape of RBCs could explain why theoretical and practical DOCs are not similar.

Our experiments showed that flow rate could be well estimated by the circular integral method of Eq. 1. The mean effect of the DOC was mainly present in the center of the tube owing to the large velocity gradient in the Z dimension at this position. Consequently, the center stream maximum speed of RBCs and velocity profiles were both directly underestimated by the DOC effect. The good precision obtained by the flow rate estimation method can be explained by the intrinsic property of the circular integral. In fact, in a flow tube if one uses the circular integral, the volume of blood in the center core represents only a small part of the total blood volume. Therefore, the circular integral method minimizes the impact of the underestimated velocities in the center core of the flow and results in good flow estimates, as in Fig. 6. Flow estimation is then a better tool to characterize physiological blood microcirculatory flows than RBC velocity vector or maximum velocity measurements.

## 5. CONCLUSIONS

Blood in microvessels is not an optimum fluid for CC applications because RBCs are non-spherical, large in size and have a large seeding volume (hematocrit). Using CC image processing approaches to measure flow of blood proved its feasibility although the DOC becomes an important factor to consider for RBCs traveling in the center stream line.

We observed in this study that the experimentally measured DOC was bigger than the theoretical one, and a nonsymmetrical aspect was also obtained. These results lead us to conclude that the theoretical measurement of DOC is

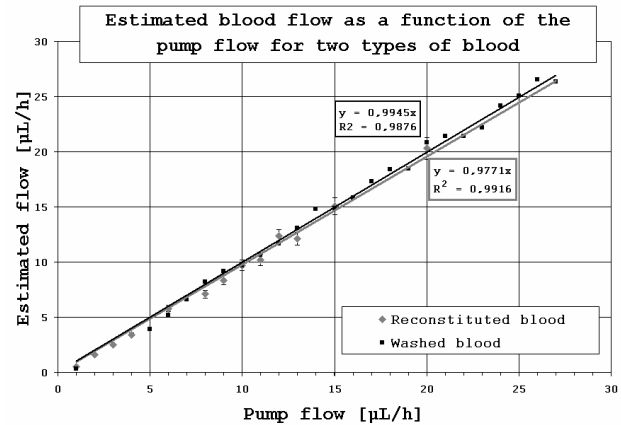


Figure 6: Blood flow estimation as a function of pump flow. Blood hematocrit was 45%, and the focus plane was set at the center of the 30  $\mu\text{m}$  diameter glass tube.

not applicable to physiological blood flow. Nevertheless, a CC algorithm can be used to compute volumic blood flow with good precision by minimizing the influence of velocity vectors affected by the large DOC.

## 6. ACKNOWLEDGMENTS

This work was supported by the NIH (#RO1HL078655), CIHR (#CMI 72323) and HSFC (#PG-05-0313). Dr Cloutier is recipient of a National Scientist Award of FRSQ and Dr de Guise holds a Canada Research Chair in Imaging and Orthopedic.

## 7. REFERENCES

- [1] Cheezum, M. K., W. F. Walker, et al., "Quantitative comparison of algorithms for tracking single fluorescent particles", *Biophys J* pp. 2378-2388, 2001
- [2] Meinhart, C. D. S.T Wereley, et al., "Volume illumination for two-dimensional particle image velocimetry", *Meas Sci Technol* pp. 809-814, 2000
- [3] Cowen, E. A. and J. K. Sveen. *PIV and Water Waves*, World Scientific, 2003
- [4] Sugii, Y., R. Okuda, et al., "Velocity measurement of both red blood cells and plasma of in vitro blood flow using high-speed micro PIV technique" *Meas Sci Technol.*, pp. 1126-1130, 2005
- [5] Ishikawa M., Sekizuka E. et al., "Measurement of RBC velocities in the rat pial arteries with an image intensified high-speed video camera system", *Microvasc Res*, pp. 166-172, 1998
- [6] Bitsch, L., L. H. Olesen, et al., "Micro particle-image velocimetry of bead suspensions and blood flows." *Exp. Fluids*, pp. 505-511, 2005
- [7] Bishop, J. J., P. R. Nance, et al., "Relationship between erythrocyte aggregate size and flow rate in skeletal muscle venules", *Am J Physiol Heart Circ Physiol*, pp. H113-H120, 2004
- [8] Fung, Y. C. (1993). *Biomechanics: Mechanical properties of living tissues*, Berlin Heidelberg, New York, 1997
- [9] Parthasarathi, A. A., S. A. Japee, et al., "Determination of red blood cell velocity by video shuttering and image analysis", *Ann Biomed Eng*, pp. 313-325, 1999